Chemical Physics 481 (2016) 34–41

Contents lists available at ScienceDirect

Chemical Physics

journal homepage: www.elsevier.com/locate/chemphys

Channel-facilitated molecular transport: The role of strength and spatial distribution of interactions

Karthik Uppulury [a,*], Anatoly B. Kolomeisky [b]

[a] Department of Chemistry, Texas Tech University, Lubbock, TX 79409, USA
[b] Department of Chemistry, Department of Chemical and Biomolecular Engineering, Center for Theoretical Biological Physics, Rice University, Houston, TX 77005, USA

ARTICLE INFO

Article history:
Available online 28 June 2016

Keywords:
Channel transport
Molecule-pore interactions
Discrete-state stochastic models
Facilitated-diffusion

ABSTRACT

Molecular transport across channels and pores is critically important for multiple natural and industrial processes. Recent advances in single-molecule techniques have allowed researchers to probe translocation through nanopores with unprecedented spatial and temporal resolution. However, our understanding of the mechanisms of channel-facilitated molecular transport is still not complete. We present a theoretical approach that investigates the role of molecular interactions in the transport through channels. It is based on the discrete-state stochastic analysis that provides a fully analytical description of this complex process. It is found that a spatial distribution of the interactions strongly influences the translocation dynamics. We predict that there is the optimal distribution that leads to the maximal flux through the channel. It is also argued that the channel transport depends on the strength of the molecule-pore interactions, on the shape of interaction potentials and on the relative contributions of entrance and diffusion processes in the system. These observations are discussed using simple physical-chemical arguments.

1. Introduction

Non-equilibrium fluxes of molecules and ions are strongly regulated in biological channels, and they are critical for cell functioning [1]. Frequently, the channel transport processes are not coupled to the consumption of any chemical energy from the hydrolysis of energy rich molecules (ATP/GTP) and they are known as passive transport processes or channel-facilitated diffusion [2,3]. These processes often occur with a high selectivity and fast translocation kinetics despite the crowded nature of cells [4–7]. Measurements from such biochemical pathways attribute the metabolite selectivity by channels to the presence of strong interaction fields between the permeating molecules and the channels. It is widely accepted that some channels have evolved to facilitate diffusion of specific molecules by tuning interactions with them and that such interactions result in an optimal molecular flux through the channels [1]. Examples include sugar transport through maltoporin channels, ATP transport through VDAC channels, penicillin transport through general bacterial porin OmpF channels and oligosaccharide transport via a bacterial porin LamB *inter alia*, all of which exhibit strong binding of the metabolites with their corresponding pores [5,7–9]. It is critically important to understand the role of these interactions in the mechanisms of biological channel-facilitated molecular fluxes.

Channel transport can be viewed as consisting of two stages: (1) First, the molecular partitioning into the channel from the bulk solution and (2) the subsequent threading through the pore to the exit. The barrier for a molecule entering into the channel in *in vivo* system is usually overcome by the potential difference across the membranes [10], whereas *in vitro* systems typically rely on external voltage driving the molecular transport [11,12]. It is widely accepted that the threading process is enhanced due to the presence of molecule-pore interactions [5,7–9]. For example, electrical channel recordings by Wolfe et al. [11] and Mohammed et al. [12] that probed the polypeptide translocation through a *αHL* channel clearly highlighted the role of molecule-pore interactions. Dwell times of the polypeptides were observed to be lower when attractive sites were employed near the channel exit, which indicated that the flux is sensitive to the spatial position of the molecule-pore interactions. Furthermore, the strength of molecule-pore interactions is shown to be a key parameter in controlling molecular flux through these channels. Molecular dynamics studies by Petrone et al. that investigated gating in a ribosome exit tunnel also revealed the existence of differential barriers for various amino acid permeating molecules [13]. Overall, the above studies underline the importance of molecular-pore interactions

* Corresponding author.
E-mail address: karthik.uppulury@gmail.com (K. Uppulury).

http://dx.doi.org/10.1016/j.chemphys.2016.06.012
0301-0104/

in the channel transport. Several theoretical models were developed to investigate channel transport by explicitly accounting for molecule-pore interactions [14–23]. However, a comprehensive understanding of the influence of molecule-pore interactions on the net flux is still unavailable due to the overall complex nature of the involved biochemical pathways.

Theoretical investigations of molecule-pore interactions in channel transport employed continuum, discrete-state and simulation approaches [14–23]. Continuum models treat molecules as diffusing particles in one dimension and evolving under a potential of mean force due to interactions between the molecules and the pore. This is frequently modeled as a symmetric square-well potential that occupies the complete volume of the channel [4,16–19]. Another approach utilizes a discrete-state stochastic formalism, which considers the volume of the channel as a finite set of discrete lattice sites/states where each lattice site accommodates a specific conformation of the molecule [20–23]. The diffusion of the molecules inside the channel can be then mapped to a single molecule performing a random walk motion on a lattice for which the dynamical quantities (such as flux, velocity and diffusion) can be solved exactly under the steady-state conditions [24]. Discrete-state approaches allow rigorous evaluation of complex spatial distributions of the molecule-pore interactions and their influence on the molecular flux. An earlier discrete-state model that accounted for molecule-pore interactions provided a good qualitative agreement [25] for the translocation kinetic data of polypeptide molecules threading a αHL channel in the presence of acidic binding sites that were positioned at different locations in the channel. However, the number of the lattice sites in the model that incorporated molecule-pore interactions was limited to only one site and the effect of its spatial orientation has been investigated. But the role of multiple binding sites with molecule-pore interactions has not been considered. While a model that considered sharply localized molecule-pore interactions provided insights into the underlying mechanisms of channel transport, the translocating molecules interact with channels everywhere, and thus it is important to probe the effect of global molecule-pore interactions. In this paper, we investigated the combined influence of multiple attractive and repulsive interactions and their spatial distributions on the channel transport. The important novelty of our approach is that both attractive and repulsive interactions are studied simultaneously. Furthermore, the influences of other factors such as load-distribution factors that affect the kinetic rates for individual transitions, size of the channel, and the numbers of special binding sites are investigated within the proposed theoretical framework.

The current model predicts: (1) a strong dependency of the channel flux on the spatial-distribution of the molecule-pore interactions as well as on the strength of the molecule-pore interactions; and (2) the existence of an optimal interaction potential between the molecules and the channel which leads to the maximal molecular flux. Significant flux enhancements are achieved via tuning the strength of molecule-pore interactions. Further, the flux dependencies on the load-distribution factors, the entry rate into the channel and the diffusion rate inside the channel also reveal the complex nature of the processes during the molecular transport through pores.

2. Theoretical method

In our model we consider a single molecule moving through the channel as shown in Fig. 1. The transport is viewed as a set of transitions between discrete states in the channel. We assume also that only one molecule can be found in the pore. There are N_0 total binding sites in the channel, of which N_a are attractive and N_r are repulsive (see Fig. 1). Hence, the sum total of special binding sites with stronger interactions N_s are equal to $N_a + N_r$. We assume that these are sites in which the molecule interacts stronger with the channel (attractively or repulsively) than at some ordinary sites. Thus, the term "attractive" or "repulsive" refers to how larger or smaller are specific interactions in comparison with the molecule-pore interactions at the ordinary sites (see Fig. 1). A molecule threading the channel interacts with each attractive (repulsive) binding site with a potential ε_a (ε_r), and at the ordinary sites we take $\varepsilon = 0$. The same zero energy is assumed for the molecule in the bulk before entering the channel. The concentration of the molecules on the left (right) of the channel is c_1 (c_2). It is important to note that the difference in the concentrations $\Delta c = c_1 - c_2$ is the main driving force for the molecular transport. Independent of the strength and location of molecule-pore interactions there will be no flux through the channel if there is no free-energy difference between the entrance and the exit. The molecules enter the channel with the rate $u_0 = k_{on}c_1$ from the left or with the rate $w_0 = k_{on}c_2$ from the right (see Fig. 1). The molecule might diffuse inside the channel from the site 'j' forwards ($j \to j+1$) and backwards ($j \to j-1$) with the rates u_j and w_j, respectively.

The probability of the molecule to be found outside the channel at time t is denoted by $P_0(t)$, and inside the channel at the site j at time t is labeled as $P_j(t)$. There is a normalization condition for all probabilities, $P_0(t) + \sum_{j=1}^{N_0} P_j(t) = 1$. The transport dynamics is controlled by the following set of Master Equations for every site j ($j = 1, 2, \ldots, N_0$) [25],

$$\frac{dP_j(t)}{dt} = u_{j-1}P_{j-1}(t) + u_{j+1}P_{j+1}(t) - (u_j + w_j)P_j(t). \quad (1)$$

The molecular flux for steady-state conditions ($t \to \infty$) has been quantified in earlier theoretical studies via mapping the transport through the channel with N_0 binding sites to a system of a single particle performing a random-walk motion periodically on a lattice with $N_0 + 1$ states (for N_0 states inside the channel and one state outside the channel) [25,26]. For example, the molecular flux in a uniform channel (when all sites are identical) is given by

$$J_0(N_0) = \frac{uu_0}{(N_0+1)\left(u + \frac{N_0}{2}u_0\right)}. \quad (2)$$

In the above situation, the uniform channel is characterized by microscopic transition rates: $u_j = w_j = u; j = 1, 2, \ldots, N_0$ that are all equal. However, generally the exit rates from the left (w_1) and the right (u_{N_0}) of the channel can differ from 'u' in the presence of molecule-channel interactions.

The one-dimensional random-walk description of the complex dynamics of molecules in the channel is obviously a simplified coarse-grained picture. However, because the channels have narrow entrance and exit regions and the molecules move in channels along effectively linear structures this approximation seems to be reasonable.

The role of molecule-pore interactions is investigated in our model by accounting for the microscopic transition rates in the presence of the 'special' (attractive or repulsive) binding sites. The free energy landscape in the presence of such special binding sites is tilted (comparing to a uniform channel) due to which the individual transition rates are also affected at these special sites. The modified chemical transition rates, specified by detailed balance, are recalculated for each chemical transition event. In what follows, the derivation of molecular flux is based on the simple assumption that the absolute value of the interaction of each of the repulsive and the attractive binding site is equal to ε. More specifically, the interactions are represented as,

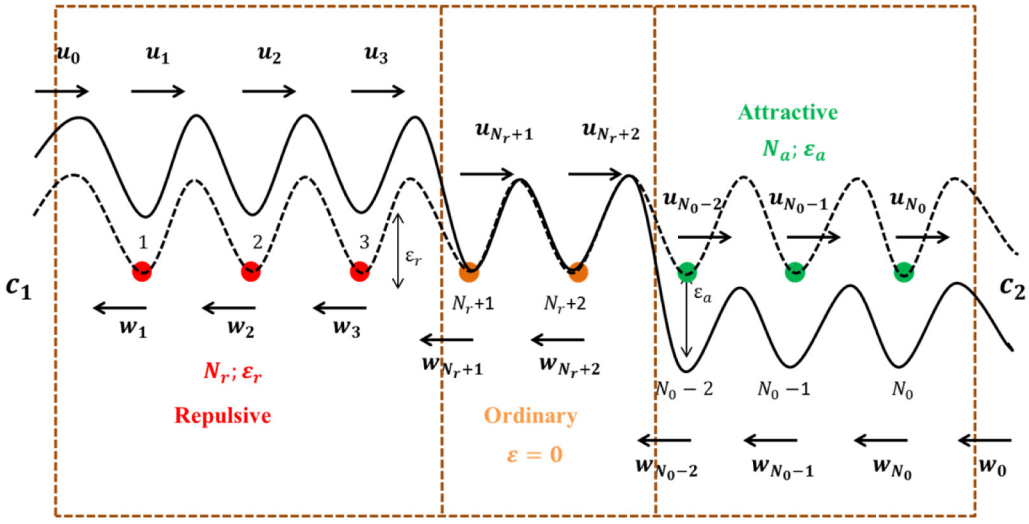

Fig. 1. Schematic of the free energy profile of molecular translocation: Channel volume is represented by the brown dotted rectangle. Binding sites are depicted in red (repulsive), orange (ordinary) and green (attractive) circles. Repulsive sites cluster at the entrance and attractive ones near the exit. There are N_r (N_a) number of repulsive (attractive) sites each of which interact with the molecules with potential ε_r (ε_a). The chemical rates of transitioning out of the site j are u_j and w_j for forward and backward transitions, respectively. The dotted curve represents a free energy profile for a channel with no interactions and the solid curve represents a landscape where molecule interacts with the channel at its respective binding site. (For interpretation of the references to color in this figure legend, the reader is referred to the web version of this article.)

$$\varepsilon_r = \varepsilon, \qquad \varepsilon_a = -\varepsilon, \quad \varepsilon > 0 \tag{3}$$

An earlier theoretical approach studied the role of interactions only for one special binding site [25]. The presented method here accounts for a more complex spatial distribution of interactions in the channel. For instance, the role of both attractive and repulsive interaction potentials is explicitly studied in the model.

It has been shown before that maximal flux is achieved in the channel when the repulsive sites cluster near the entrance and attractive sites cluster near the exit [25]. The current model here employs such an arrangement of the special binding sites. Hence, the non-special/ordinary sites are positioned in between the attractive and repulsive sites (see Fig. 1). For a channel of constant size (N_0 sites) and constant number of special sites ($N_s = N_a + N_r$; note that $N_a and N_r$ may vary but N_s is fixed), there exist many combinatorial possibilities of spatially distributing the special sites. All possible scenarios are classified into four distinct cases based on the number of non-special/ordinary binding sites (N_{ns}) in the channel. These consist of: (i) $N_{ns} = 0$, (ii) $N_{ns} = 1$, (iii) $N_{ns} = 2$ and (iv) $N_{ns} \geqslant 3$. Although each of the cases $N_{ns} = 0, 1, 2$ can be described by a unique set of Master equations, leading to a unique expression for flux, we analyze only the situation of $N_{ns} \geqslant 3$ here since it represents the most generic case. It is expected that the underlying mechanistic implications from this case will still hold true for the former three cases as well.

In each of the above four situations, the analytical expressions for flux inside the channel is distinct due to the 'edge' effects (between the special and non-special binding sites) across the regions of (a) repulsive and non-special sites and (b) non-special and attractive sites. The flux in the four classified systems above changes due to the fact that the chemical rates connecting the special and non-special binding sites in each of the above scenario will alter the overall flux across the channel.

2.1. Detailed balance-like conditions

The chemical reaction rates (k) for the molecule hopping across the binding sites in the channel can be expressed in terms of the general Arrhenius expressions as $k = Ae^{-\beta E_{act}}$, where E_{act} is the activation barrier, β equals $(k_B T)^{-1}$ with k_B being the Boltzmann constant, T is the temperature and A is the pre-exponential factor. For a uniform channel with no special molecule-channel interactions the pre-exponential factor corresponds to the diffusion rate 'u' inside the channel. It is expected that interactions will modify the transition rates as described below.

For the case of $N_{ns} \geqslant 3$ the modified chemical transition rates specified by the detailed balance-like conditions are represented in Eqs. 4–6 for the repulsive sites and in Eqs. 7–10 for the attractive sites:

$$\frac{u_0}{w_1} = \frac{u_0^0}{w_1^0}.e^{\beta(0-\varepsilon_r)} = \frac{u_0^0}{w_1^0}.e^{-\beta\varepsilon} \tag{4}$$

$$\frac{u_1}{w_2} = \frac{u_1^0}{w_2^0}.e^{\beta(\varepsilon_r-\varepsilon_r)} = \frac{u_1^0}{w_2^0}.e^{\beta(\varepsilon-\varepsilon)} \tag{5}$$

$$\frac{u_{N_r}}{w_{N_{r+1}}} = \frac{u_{N_r}^0}{w_{N_r+1}^0}.e^{\beta(\varepsilon_r-0)} = \frac{u_{N_r}^0}{w_{N_r+1}^0}.e^{\beta(\varepsilon-0)} \tag{6}$$

$$\frac{u_{N_0-N_a}}{w_{N_0-N_a+1}} = \frac{u_{N_0-N_a}^0}{w_{N_0-N_a+1}^0}.e^{\beta(0-\varepsilon_a)} = \frac{u_{N_0-N_a}^0}{w_{N_0-N_a+1}^0}.e^{\beta(\varepsilon)} \tag{7}$$

$$\frac{u_{N_0-N_a+1}}{w_{N_0-N_a+2}} = \frac{u_{N_0-N_a+1}^0}{w_{N_0-N_a+2}^0}.e^{\beta(\varepsilon_a-\varepsilon_a)} = \frac{u_{N_0-N_a+1}^0}{w_{N_0-N_a+2}^0}.e^{\beta(-\varepsilon+\varepsilon)} \tag{8}$$

$$\frac{u_{N_0-1}}{w_{N_0}} = \frac{u_{N_0-1}^0}{w_{N_0}^0}.e^{\beta(\varepsilon_a-\varepsilon_a)} = \frac{u_{N_0-1}^0}{w_{N_0}^0}.e^{\beta(-\varepsilon+\varepsilon)} \tag{9}$$

$$u_{N_0} = u_{N_0}^0.e^{\beta(\varepsilon_a-0)\theta} = u_{N_0}^0.e^{-\beta(\varepsilon)\theta} \tag{10}$$

The complete set of detailed balance equations is not written here, but it is straightforward to do it. The physical meaning of these expressions is the fact that interactions change the free-energy difference between two states connected by the transition, which is given by the ratio of corresponding forward and backward transition rates.

2.2. Microscopic rates

To obtain the full dynamic description of the molecular transport through channels explicit expressions for transition rates are needed. This can be obtained from the detailed balance-like arguments by introducing a parameter 'θ' – the load distribution factor [25]. The distribution factor 'θ' represents the position of the transition state (TS) for a chemical transition event along the molecule's reaction coordinate. The load-distribution factor depicts how the (molecule-pore) interaction energy is distributed between the forward and the backward transition rates. The individual forward and backward rates are expressed in Eqs.11–21. An assumption of $w_0 = 0$ is made which simplifies the final analytical form of the molecular flux.

$$u_0 = u_0^0 e^{-\beta\varepsilon_r\theta} = u_0^0 e^{\beta\varepsilon\theta} \tag{11}$$

$$u_i = u_i^0 = u; \quad i = 2,3,4,\ldots,N_r - 1 \tag{12}$$

$$u_{N_r} = u_{N_r}^0 e^{\beta\varepsilon_r\theta} = u_{N_r}^0 e^{-\beta\varepsilon\theta} \tag{13}$$

$$w_1 = w_1^0 e^{-\beta\varepsilon_r(\theta-1)} = w_1^0 e^{\beta\varepsilon(\theta-1)} \tag{14}$$

$$w_i = w_i^0 = u; \quad i = 2,3,4,\ldots,N_r - 1 \tag{15}$$

$$w_{N_r+1} = w_{N_r+1}^0 e^{\beta\varepsilon_r(\theta-1)} = w_{N_r+1}^0 e^{-\beta\varepsilon(\theta-1)} \tag{16}$$

$$u_{N_0-N_a} = u_{N_0-N_a}^0 e^{-\beta\varepsilon_a\theta} = u_{N_0-N_a}^0 e^{\beta\varepsilon\theta} \tag{17}$$

$$u_i = u_i^0 = u; \quad i = N_0 - N_a + 1,\ldots,N_0 - 1 \tag{18}$$

$$u_{N_0} = u_{N_0}^0 e^{\beta\varepsilon_a\theta} = u_{N_0}^0 e^{-\beta\varepsilon\theta} \tag{19}$$

$$w_{N_0-N_a+1} = w_{N_0-N_a+1}^0 e^{-\beta\varepsilon_a(\theta-1)} = w_{N_0-N_a+1}^0 e^{\beta\varepsilon(\theta-1)} \tag{20}$$

$$w_i = w_i^0 = u; \quad i = N_0 - N_a + 2,\ldots,N_0 \tag{21}$$

$$w_0 = 0 \tag{22}$$

2.3. Molecular flux

The molecular flux, J, in the channel is calculated using Eq. S1 (see SI and the derivations therein) by accounting the modified chemical rates and is given as follows:

$$J = \frac{uu_0}{uA + u_0 B} \tag{23}$$

$$A = 1 + e^{-\beta\varepsilon} + e^{-2\beta\varepsilon\theta} + (N_a - 1)e^{-\beta\varepsilon(\theta+1)} + e^{-\beta\varepsilon(2\theta-1)} + (N_r - 1)e^{-\beta\varepsilon(\theta-1)} + (N_0 - N - 1)e^{-\beta\varepsilon\theta} \tag{24}$$

$$B = \frac{N_a}{2}(N_a - 1) + \frac{N_r}{2}(N_r - 1) + \frac{N_0 - N}{2}(N_0 - N - 1) + N_r(N_a - 1)e^{-2\beta\varepsilon} + (N_0 - N_a)e^{-\beta\varepsilon\theta} + N_r e^{-\beta\varepsilon(\theta+1)} + N_r e^{\beta\varepsilon(\theta-2)} + (N_0 - N)e^{\beta\varepsilon(\theta-1)} + (N_a - 1)e^{\beta\varepsilon\theta} + e^{-\beta\varepsilon(\theta-1)} + ((N_0 - N - 1)(N - 2) + N_0 - N_r - 2)e^{-\beta\varepsilon} \tag{25}$$

It can be verified that $\frac{J}{J_0} = 1$ for the uniform channel with no (molecule-pore) interactions i.e., when the system parameters are: $N_a = N_r = 0$; $N = N_s = 0$; $\varepsilon = 0$; $\theta = 0$. Thus, Eqs. (23)–(25) provided are explicit expressions for the molecular flux through the channels, and they can be effectively analyzed to understand the role of interactions.

2.4. Optimal binding sites

Eqs. 23–25 suggest that the molecular flux depends on system parameters such as the channel size, the number of special binding sites, the diffusion rates, distribution factor and the molecule-pore interactions. The flux dependence on the number of special sites and the relative partition of attractive and repulsive binding sites can be easily calculated. More specifically the optimal number of sites (N_a^*, N_r^*) for a channel of the fixed length and the fixed number of special lattice sites (N_s) can be analytically evaluated. The expression for the optimal number of attractive (N_a^*) sites is obtained from the condition: $\frac{\partial J}{\partial N_a}\big|_{N_0,N_s} = 0$. This leads to the following analytic expression to obtain N_a^* needed for the maximal flux through the channel.

$$N_a^* = \frac{u}{u_0}\left[\frac{e^{-\beta\varepsilon(\theta-1)} - e^{-\beta\varepsilon(\theta+1)}}{2(1 - e^{-2\beta\varepsilon})}\right] + \left[\frac{N - (N+1)e^{-2\beta\varepsilon} + e^{-\beta\varepsilon\theta} + e^{\beta\varepsilon(\theta+1)} + e^{\beta\varepsilon(\theta-2)} - e^{\beta\varepsilon\theta} - e^{-\beta\varepsilon}}{2(1 - e^{-2\beta\varepsilon})}\right] \tag{26}$$

The optimal number of repulsive binding sites is simply obtained via: $N_r^* = N_s - N_a^*$.

3. Results and discussions

3.1. Role of molecule-channel interaction strength

In order to understand the transport mechanisms and the factors that govern the current through the pores, in Figs. 2 and 3 we present the channel flux dependence on the number of molecule-pore interactions and their strength. Using Eq. (23), the normalized current through the channel (J/J_0) is calculated for

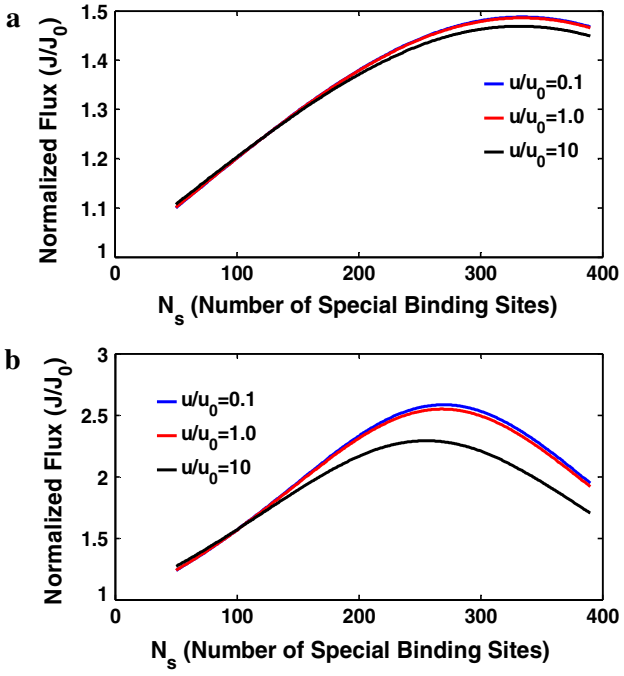

Fig. 2. The normalized flux (J/J_0) versus number of special sites is presented. A channel with $N_0 = 400$ binding sites and load-distribution factor $\theta = 0.5$ is considered. (a) $\varepsilon = 0.5k_BT$ and (b) $\varepsilon = 3k_BT$. The blue, red and black solid lines in (a) and (b) represent u/u_0 equal to 0.10, 1.0 and 10.0 respectively. (For interpretation of the references to color in this figure legend, the reader is referred to the web version of this article.)

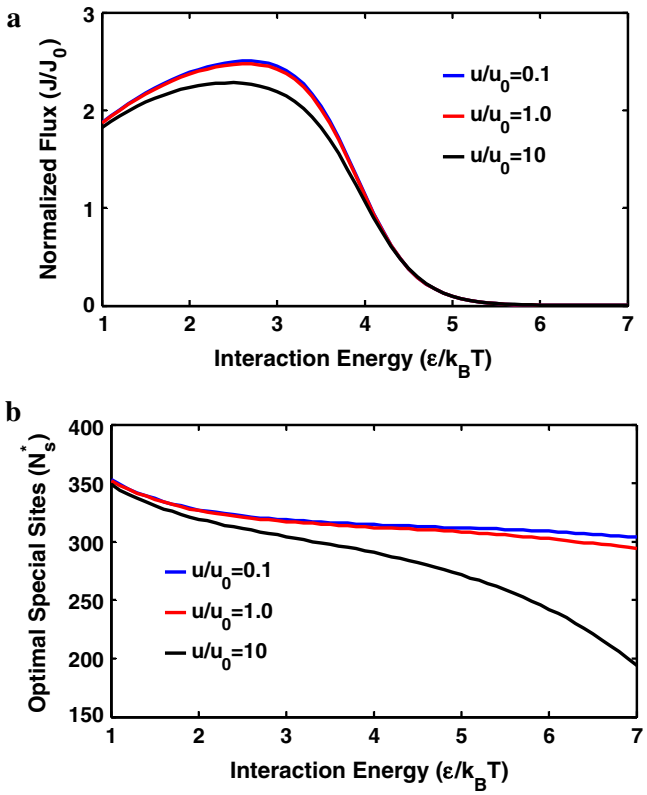

Fig. 3. (a) The normalized flux as a function of the molecule-channel strength (b) The optimal number of special sites as a function of molecule-pore interaction energy is shown. A channel with $N_0 = 400$ binding sites and load distribution factor $\theta = 0.5$ is considered. The blue, red and black solid curves correspond to u/u_0 equal to 0.1, 1.0 and 10.0 respectively. (For interpretation of the references to color in this figure legend, the reader is referred to the web version of this article.)

several sets of parameters. First, the flux dependence with respect to the total number of the molecule-pore interactions, N_s, is investigated (Fig. 2). A channel with $N_0 = 400$ binding sites was analyzed. Repulsive binding sites are clustered at the entrance and the attractive sites are near the exit of the channel such that $N_a + N_r = N_s$. For a channel with the fixed size (N_0) and with the fixed number of special sites (N_s), the optimal number of attractive binding sites (N_a^*) is given by Eq. (26). N_a^* is plugged into Eq. (23) to calculate the flux for a given set of system parameters. A load-distribution factor of 0.5 is assumed, but the results do not depend much on varying this parameter (see below). To understand the flux sensitivity to molecule-pore interactions, the normalized flux (J/J_0) versus N_s is calculated for systems with $\varepsilon = 0.5k_BT$ (Fig. 2a) and $\varepsilon = 3k_BT$ (Fig. 2b). Here, ε is simply the absolute value of the interaction potential of the attractive/repulsive binding site but the flux contains the combined effect of the repulsive sites (near the entrance) and the attractive sites (near the exit). The blue, red and black curves in Fig. 2a,b correspond to various ratios of diffusion over the entrance rates, u/u_0, equal to 0.1, 1.0 and 10 respectively ($\theta = 0.5$ in all cases). Clearly, the normalized flux reaches a maximum in Fig. 2a,b for some optimal number of the special binding sites, N_s^*, which varies with the molecule-pore interaction strength. The percent increase in the maximal flux $\left(\left(\frac{J}{J_0} - 1\right) \times 100\%\right)$ is ~50% when $\varepsilon = 0.5k_BT$ (Fig. 2a) and is ~160% when $\varepsilon = 3.0k_BT$ (Fig. 2b) compared to the uniform channel.

Our results suggest that for weak interactions ($\varepsilon = 0.5k_BT$) larger number of binding sites is necessary in order to reach the maximal flux in comparison with the case of stronger interactions ($\varepsilon = 3.0k_BT$). Calculations suggest that $N_s^* \sim 350$ when $\varepsilon = 0.5k_BT$ (Fig. 2a) and ~260 when $\varepsilon = 3k_BT$ (Fig. 2b). So, for a relatively high ε the optimal number of special sites (N_s^*) required for maximal flux is lower, i.e., the peak for optimal N_s in Fig. 2a ($\varepsilon = 0.5k_BT$) shifts to the left when ε is increased. Hence it is argued that the flux is sensitive to the total strength of the molecule-pore interactions (N_s). Modifying N_s correlates with the spatial organization of attractive and repulsive binding sites. Overall, results from Fig. 2 strongly support the idea that the flux is sensitive to the total strength of molecule-pore interactions in the channel and that the molecular flux can be expedited significantly by varying the molecule-pore interactions.

To better understand the flux dependency on the molecule-pore interaction strength (ε), the possibility for the optimal interaction strength is explored. In order to achieve this, the normalized flux is calculated for varying strengths of molecule-pore interactions. It is estimated for a channel ($N_0 = 400$) with attractive sites clustered near the exit and the repulsive sites near the entrance. A load-distribution factor of $\theta = 0.5$ is assumed. The plots in Fig. 3a reveal the existence of the optimal interaction strength (ε^*) between the molecules and the channel. Specifically, an interaction strength of $\varepsilon^* \sim 3k_BT$ achieves the maximal flux in the channel. For interaction potentials with $\varepsilon < \varepsilon^*$ and $\varepsilon > \varepsilon^*$ the flux is lower, and J/J_0 decreases rapidly as the interaction strength increases to $\sim 5k_BT$. The increase in the strength of interactions imposes higher enthalpic barriers for an incoming molecule to surmount thereby lowering its probability to translocate. Apparently, the flux in the system vanishes for relatively high molecule-pore interaction strengths. Fig. 3a displays ratio of fluxes for varying values of u/u_0 equal to 0.1 (blue curve), 1.0 (red curve) and 10.0 (black curve). The flux is similar for the cases of u/u_0 equal to 0.1 and 1.0. For the case of $u/u_0 = 10$ (black curve) the maximal flux is lower compared to the blue and red curves. A higher ratio of u/u_0 implies lowered u_0 meaning that the entry rate into the channel from the entrance of the pore is lower compared to the scenario of $u/u_0 = 0.1$. In Fig. 3b, the number of optimal special sites (N_s^*) is calculated in a channel ($N_0 = 400$, $\theta = 0.5$) with respect to the interaction potential for maximal flux conditions. It can be seen that for relatively weak strengths (ε), the molecule-pore interactions tend to occupy the whole volume of the channel (large N_s^* is predicted) and N_s^* decreases with increase in the strength of interactions. The plots in Fig. 3b correspond to varying u/u_0 and reveal the sensitivity of N_s^* to the ratio of diffusion rates to the entrance rates. For the case of $u/u_0 = 10$ fewer optimal binding sites are needed with increasing interaction strength for optimal flux. This trend can be rationalized by the arguing that a system with higher u/u_0 provides molecules with greater thrust or higher diffusion rate u inside the channel to permeate the channel (owing to native chemical interactions with the channel) thus requiring fewer energetic gains from the interactions with the special sites. Similar trends are seen for $-u/u_0 = 1.0, 0.1$.

3.2. Role of spatial orientation of molecule-channel interactions

The spatial organization of the special binding sites is another control parameter for maximal flux that can be investigated. A channel with constant number special sites has many combinatorial possibilities of arranging the attractive and repulsive sites (given the criterion: $N_a + N_r = N_s$). This leads to the task of predicting the most probable combination/partition of the special sites for which the corresponding free energy landscape will yield the optimal flux through the channels. To understand the role of spatial distribution of the special sites, the binding site fractions $\frac{N_a}{N_s}$, $\frac{N_r}{N_s}$ of the attractive and repulsive sites are calculated, and the results are presented in Fig. 4. To illustrate this, a channel with $N_0 = 400$ and $N_s = 300$ special sites is considered. A load-distribution factor of $\theta = 0.5$ is chosen for all transitions. The site fractions are then

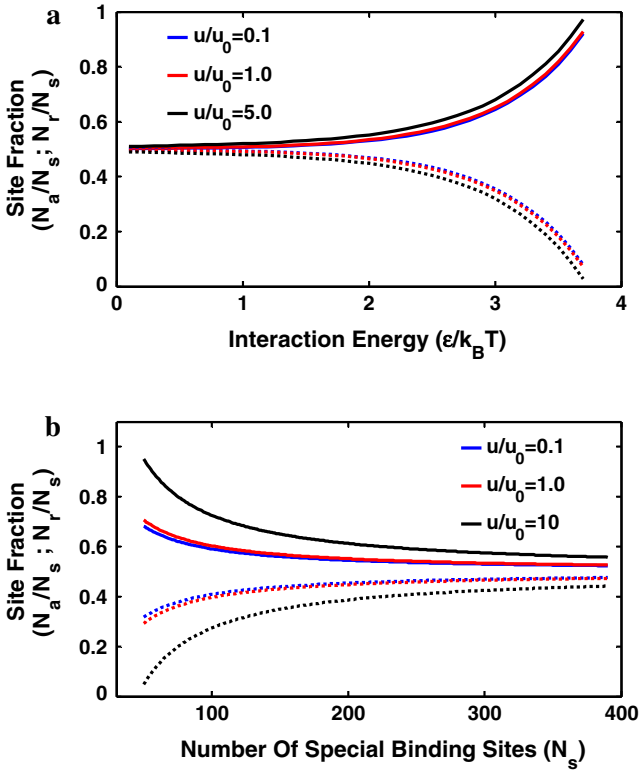

Fig. 4. The fractions of attractive and repulsive sites are calculated with respect to the (a) interaction energy and the (b) number of special sites. A channel with $N_0 = 400$ binding sites, $N_s = 300$ and load distribution factor $\theta = 0.5$ is considered. Solid lines represent the attractive site fractions whereas the dotted lines represent the repulsive site fractions. The blue and red curves represent u/u_0 equal to 0.1 and 1.0 respectively. The black curve corresponds to u/u_0 equal to 5.0 in (a) and 10.0 in (b). The interaction energy is $\varepsilon = 2k_BT$ in (b). (For interpretation of the references to color in this figure legend, the reader is referred to the web version of this article.)

evaluated for varying molecule-pore interaction strengths. For relatively weak interaction potentials, the site fractions are almost equal. As the interaction strength increases, the site fractions are modified such that the fraction of attractive sites increases and the fraction of the repulsive sites decreases. This trend is due to the spatial positioning of these sites. Since the repulsive sites cluster near the entrance, a strong interaction strength (ε) will impose a higher barrier for the molecular entering into the channel, thereby reducing the flux. Hence, fewer repulsive sites are optimal. As a consequence, relatively more attractive sites are needed to overcome the effect of the repulsive sites and to successfully translocate the molecules through the channel. Thus, the interplay of the attractive and repulsive sites (for optimal transport) is strongly correlated with the molecule-pore interaction strength – stronger the interaction strength, the greater will be the number of attractive sites employed. Plots in Fig. 4a correspond to u/u_0 = 0.1 (blue), 1.0 (red) and 5.0 (black). The site fractions are less sensitive to the variations in u/u_0 for lower values (<1.0). As u/u_0 increases the attractive site fraction increases for e.g. $u/u_0 = 5$. This can be rationalized by the argument that increasing u/u_0 implies lowered u_0 which essentially lowers the molecular flux to entering the channel. So in order to expedite the molecular flow the number of attractive sites utilized to achieve optimal flux must be increased. However, these increments are relatively modest for an increase of u/u_0 from 0.1, 1.0 (blue, red solid lines) to 5 (black solid) as shown in Fig. 4a. Overall, it is evident that the molecule-pore interactions modify the free energy landscape in a way that dictates some optimal partition between the attractive and repulsive bindingites to achieve optimal flux through the channel.

To further understand the influence of spatial distribution of special sites, the site fractions are calculated with respect to number of special sites (N_s). In this scenario, the molecule-pore interaction strength is fixed and the number of special sites is varied. A channel ($N_0 = 400$) with interaction strength of $\varepsilon = 2k_BT$ and load-distribution factor $\theta = 0.5$ is considered. Calculations from Fig. 4b show that for fewer number of special binding sites employed in the channel the number of the molecule-pore interactions is dominated by the attractive interactions. The predicted higher attractive binding site fraction (solid lines in Fig. 4b) can be understood as follows. Let us consider the case of fewer special sites with significant number of them repulsive in nature then there will be an entropic penalty for the molecules to partition into the channel and eventually to translocate. The barriers to allow molecules to partition into the channel can be overcome if relatively more attractive sites are employed. This will not only allow easier molecular partitioning into the channel but it will also enhance the molecular flow due to greater number of attractive sites at the exit of the channel. As the number of the special binding sites increases (close to the size of the channel), they influence the tilting of the free energy landscape to allow the partition of the attractive and repulsive binding sites to produce the maximal molecular current in the channel. The curves in Fig. 4b show the site fractions for varying diffusion and entrance rates, u/u_0. Less sensitivity is observed for lower values of $u/u_0(0.1, 1.0)$. Again, the site fraction is seen to be sensitive at higher values of u/u_0. The attractive site fraction for $u/u_0 = 10$ (solid black) is higher compared to the case of $u/u_0 = 0.1, 1.0$ (solid blue, red lines). This can be rationalized once again by the argument that a higher value of u/u_0 implies a lower value of u_0 which leads to a lower molecular flux across the channels. In order to enhance the flux, a greater fraction of attractive sites is optimal for higher u/u_0 ($u/u_0 = 10$, black solid line) than compared to the low values of u/u_0 (0.1, 1.0; blue, red solid lines). Overall, these results suggest that the optimal spatial organization of the attractive and repulsive sites for maximal flux depends both on the molecule-pore interactions and on the fraction $\left(\frac{N_s}{N_0}\right)$ of the special sites with interactions.

Next, the site fraction dependency on the load-distribution factor (θ) is evaluated. The load-distribution factor dictates the shape of the molecule-pore interactions – it relates to the position of transition state (TS) along the reaction coordinate. A relatively low value indicates the TS position closer to the initial configuration whereas a higher value indicates its proximity to the final configuration. A channel with $N_0 = 400$ sites, $N_s = 300$ special sites and molecule-pore strength $\varepsilon = 2k_BT$ is analyzed. As the load-distribution factor increases the fraction of attractive sites also increases (Fig. 5a). A higher θ lowers the net forward transition rate of the microscopic transitions which slows down the molecular flux. It is predicted that with increasing the load-distribution factors the fraction of attractive sites has to increase for maximal flux. This is intuitively clear since the attractive sites are placed near the channel exit at which location they increase the probability of the molecular flux. The site fractions are calculated for varying u/u_0. The variations in site fractions are less sensitive to u/u_0 at lower values ($u/u_0 = 0.1$, 1.0 – blue and red lines). However, the trend is interesting for $u/u_0 = 10$ (black solid and dotted lines), for which there is an initial decrease in the attractive site (black solid line, Fig. 5a) fraction (with increase in load-distribution factor) and then increases with the load-distribution factor. This can be understood from the specific situation of $u/u_0 = 5$ in Fig. 5b, where the attractive site fraction initially decreases (solid blue line, Fig. 5b) with increase in the load-distribution factor and then increases for the higher load-distribution factors. This feature can be explained by the effect of two competing factors, such as the diffusion rate (u) and the load-distribution factor (θ). For $\theta < 0.5$ the transport

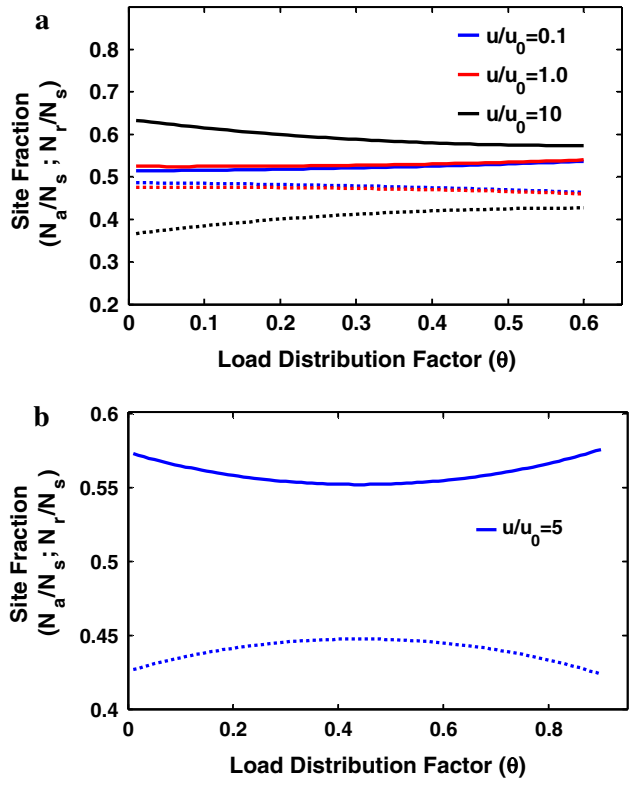

Fig. 5. Site fractions are calculated with respect to the load-distribution factor. A channel with $N_0 = 400$ binding sites, $N_s = 300$ binding sites and $\varepsilon = 2k_BT$ is considered. (a) The blue, red and black curves depict site fractions with u/u_0 equal to 0.1, 1 and 10 respectively. (b) The blue curves depict site fractions for u/u_0 equal to 5. The solid lines correspond to attractive site fractions and dotted ones correspond to repulsive ones. (For interpretation of the references to color in this figure legend, the reader is referred to the web version of this article.)

process is likely to be more dependent on a higher diffusion rate. This requires fewer attractive binding sites compared to the regime where $\theta > 0.5$ which follows similar trends with respect to the load-distribution factor as in $u/u_0 = 0.1, 1.0$ in that more attractive sites are needed to drive transport. Overall, the molecular flux dependency on the load-distribution factor is predicted to be governed by competing factors of the diffusion rates inside the channel and the channel entry rate.

4. Conclusions

In conclusion, the channel-facilitated molecular transport is studied by considering the role of the spatial distribution and the strength of the molecule-pore interactions. The presence of interactions influences the overall free energy landscape in the molecule's translocation through the channel. Specifically, our findings can be summarized as follows (1a) it is clearly shown that the molecular flux in the channel is strongly dependent on the strength of the molecule-pore interactions and (1b) that there exists an optimal interaction potential between molecules and the pore that yields maximal flux in the channel.

(2) The effect of the total number of the molecule-pore interactions on the channel transport is analyzed. It is found that for weaker interactions relatively greater (number of) special binding sites are needed, whereas for stronger interactions lesser special binding sites are required for the optimal flux conditions.

(3) We also find that there is an optimal partitioning between the attractive and repulsive sites that maximizes the molecular flux in the channel.

(4) The model also investigated the effect of variations on the total number of molecule-pore interactions. It is revealed that in the system with few special sites more attractive sites should be employed and with increasing the number of special sites the fractions of attractive and repulsive sites should be similar.

(5) Finally, the site fraction dependency with respect to the load-distribution factor revealed a complex relationship and it is found that competing factors of the diffusion rate inside the channel and the entry rate at various load-distribution factors influence the molecular transport.

Recent simulation studies pertinent to ribosomal exit channels reported existence of differential energy barriers ($\sim 2 - 7k_BT$, attractive in nature) for various amino acids near the channel exit and corroborate the feature of channel specificity to certain type of metabolites [13]. The interaction energies explored in this article as well are in a similar energy range and that the existence of an optimal interaction between the molecules and the pore predicted within the model framework agrees well with the simulation studies and experimental measurements. The true free energy landscape for molecular transport depends on the nature of the metabolites and channels and other environmental parameters. Although more advanced theoretical and computational models are needed in the future, the current theoretical framework can address and predict channel transport properties and it can also clarify the underlying mechanisms.

Conflict of interest

There is no conflict of interest.

Acknowledgement

ABK acknowledges the support from the Welch Foundation (Grant C-1559).

Appendix A. Supplementary data

Supplementary data associated with this article can be found, in the online version, at http://dx.doi.org/10.1016/j.chemphys.2016.06.012.

References

[1] A. Meller, J. Phys.: Condens. Matter. 15 (2003) R581–R607.
[2] W. Wickner, R. Schekman, Science 310 (2005) 1452–1456.
[3] H. Lodish, A. Berk, S.L. Zipursky, P. Matsudaira, D. Baltimore, J. Damell, Molecular Cell Biology, fourth ed., Freeman, New York, 2002.
[4] A.M. Berezhkovskii, S.M. Bezrukov, Chem. Phys. 319 (2005) 342–349.
[5] T.K. Rostovtseva, S.M. Bezrukov, Biophys. J. 74 (1998) 2365–2373.
[6] M. Luckey, H. Nikaido, Proc. Natl. Acad. Sci. U.S.A. 77 (1980) 167–171.
[7] R. Benz, A. Schmid, G.H. Vos-Scheperkeuter, J. Membr. Biol. 100 (1987) 21–29.
[8] S.M. Bezrukov, L. Kullman, M. Winterhalter, FEBS Lett. 476 (2000) 224–228.
[9] E.M. Nestrovich, C. Danelon, M. Winterhalter, S.M. Bezrukov, Proc. Nat. Acad. Sci. 99 (2002) 9789–9794.
[10] F. Bezanilla, Nat. Rev. Mol. Cell Biol. 9 (2008) 323–332.
[11] A.J. Wolfe, M.M. Mohammed, S. Cheley, H. Bayley, L. Movileanu, J. Am. Chem. Soc. 129 (2007) 14034–14041.
[12] M.M. Mohammed, S. Prakash, A. Matouschek, L. Movileanu, J. Am. Chem. Soc. 130 (2008) 4081–4088.
[13] P.M. Petrone, C.D. Snow, D. Lucent, V.S. Pande, Proc. Nat. Acad. Sci. 105 (2008) 16549–16554.
[14] T. Chou, Phys. Rev. Lett. 80 (1998) 85–88.
[15] T. Chou, J. Chem. Phys. 110 (1999) 606–615.
[16] A.M. Berezhkovskii, M.A. Pustovoit, S.M. Bezrukov, J. Chem. Phys. 116 (2002) 9952–9956.

[17] A.M. Berezhkovskii, M.A. Pustovoit, S.M. Bezrukov, J. Chem. Phys. 119 (2003) 3943–3951.
[18] A.M. Berezhkovskii, S.M. Bezrukov, Biophys. J. 88 (2005) L17–L19.
[19] S.M. Bezrukov, A.M. Berezhkovskii, A. Szabo, J. Chem. Phys. 127 (2007) 115101.
[20] A.B. Kolomeisky, Phys. Rev. Lett. 98 (2007) 048105.
[21] A.B. Kolomeisky, S. Kotsev, J. Chem. Phys. 128 (2008) 085101.
[22] A. Zilman, Biophys. J. 96 (2009) 1235–1248.
[23] A. Zilman, J. Pearson, G. Bel, Phys. Rev. Lett. 103 (2009) 128103.
[24] A.B. Kolomeisky, E. Stukalin, A.A. Popov, Phys. Rev. E. 71 (2005) 031902.
[25] A.B. Kolomeisky, K. Uppulury, J. Stat. Phys. 142 (2011) 1268–1276.
[26] B. Derrida, J. Stat. Phys. 31 (1983) 433–450.